J. Mol. Biol. (1994) 236, 831–843

The 1·9 Å Structure of Deoxyβ_4 Hemoglobin

Analysis of the Partitioning of Quaternary-associated and Ligand-induced Changes in Tertiary Structure

Gloria E. O. Borgstahl†, Paul H. Rogers and Arthur Arnone‡

Department of Biochemistry, The University of Iowa, Iowa City, IA 52242, U.S.A.

The crystal structure of the deoxygenated form of the human hemoglobin β_4 tetramer (deoxyβ_4) has been determined and refined at a resolution of 1·9 Å. A detailed comparison of the quaternary structures of carbonmonoxy-β_4 (COβ_4) and deoxyβ_4 shows that ligand binding to the β_4 tetramer produces only slight movements of the subunits relative to each other. Therefore, unlike the hemoglobin $\alpha_2\beta_2$ tetramer, where the transition from an unliganded T state tetramer to a liganded R state tetramer results in a large change in quaternary structure, β_4 is locked in a quaternary structure that very closely resembles the R state. By comparing the high-resolution structures of T state deoxy $\alpha_2\beta_2$, R state deoxyβ_4 and R state COβ_4, it is possible to partition the changes in β subunit tertiary structure into those that arise from changes in quaternary structure and those that result solely from ligand binding. Specifically, when viewed from the heme reference frame, comparison of the structures of T state deoxy $\alpha_2\beta_2$ and R state deoxyβ_4 shows that the T-to-R quaternary structure transition induces changes in β subunit tertiary structure that are approximately halfway toward the tertiary structure observed in liganded β_4 and liganded $\alpha_2\beta_2$. When viewed from the reference frame of the globin backbone atoms, the T-to-R quaternary structure transition induces a small rotation of the heme group and a shift of the "allosteric core" (the end of the F helix, the FG corner, the beginning of the G helix, and the heme group) away from the E helix. These movements open the ligand binding pocket and place the heme in a more symmetric position relative to the proximal histidine residue. Together, these effects work in unison to give the subunits of deoxyβ_4 a tertiary structure that has high ligand affinity.

Keywords: X-ray crystal structure; hemoglobin; R state; ligation intermediate; allostery

1. Introduction

The binding of ligand to hemoglobin (Hb§), an $\alpha_2\beta_2$ tetramer, results in a large change in quaternary structure as well as smaller changes in the tertiary structure (Perutz, 1970; Baldwin & Chothia, 1979). Only one structure, the T state (Fermi *et al.*, 1984), has been observed for the deoxy $\alpha_2\beta_2$ tetramer, whereas there are two known structures for fully liganded Hb, the R state (Shaanan, 1983) and the R2 state (Silva *et al.*, 1992). In the accompanying paper (Borgstahl *et al.*, 1993), it is demonstrated that the quaternary and tertiary structures of carbonmonoxy-β_4 (COβ_4) are very similar to those of the liganded $\alpha_2\beta_2$ R state tetramer. Here we show that, unlike the $\alpha_2\beta_2$ tetramer, ligand binding induces very little change in β_4 quaternary structure. Therefore, the structure of deoxygenated β_4 (deoxyβ_4) serves as a model for the R state of deoxyHb, a form of the $\alpha_2\beta_2$ tetramer that is present in extremely small amounts and is very difficult to study.

The full deoxy T state to liganded R state transition can be partitioned into a deoxy T state to deoxy R state transition followed by a deoxy R state to liganded R state transition. Changes in subunit tertiary structure that result from the first transition are solely due to differences in quaternary structure (i.e. differences in subunit-subunit interactions), whereas the changes in tertiary structure that result from the second transition are solely due to the effects of ligand binding. By using deoxyβ_4 as

† Present address: The Scripps Research Institute, La Jolla, CA 92037, U.S.A.

‡ Author to whom all correspondence should be addressed.

§ Abbreviations used: Hb, hemoglobin; oxyHb(R), R state oxy $\alpha_2\beta_2$ Hb; deoxyHb(T), T state deoxy $\alpha_2\beta_2$ Hb; COHb(R2), R2 state carbonmonoxy $\alpha_2\beta_2$ Hb; deoxyβ_4(R), R state deoxy β_4 Hb; COβ_4(R), R state carbonmonoxy β_4 Hb; r.m.s., root-mean-square; BME, bis(*N*-maleimidomethyl).

0022–2836/94/080831–13 $08.00/0

a model for the deoxy $\alpha_2\beta_2$ R state, it is possible to partition the changes in β subunit tertiary structure that are associated with the full T-to-R transition into quaternary-associated changes and ligand-induced changes.

2. Materials and Methods

(a) *Collection of diffraction data*

Deoxyβ_4 crystallizes under conditions that are similar to those described for COβ_4 (Arnone & Briley, 1978). Specifically, batch crystallization solutions were prepared in a nitrogen-filled glove box and consisted of 1% Hb, 2·04 M sulfate, 0·26 M phosphate and 9 mM ferrous citrate. Deoxyβ_4 crystals belong to the space group $P2_1$ with $a = 63{\cdot}0$ Å, $b = 81{\cdot}8$ Å, $c = 54{\cdot}4$ Å and $\beta = 89{\cdot}7°$. Diffraction data were collected as described (Borgstahl *et al.*, 1993) using 2 crystals mounted in quartz capillaries under an atmosphere of pure nitrogen. A total of 46,515 unique reflections were collected (352,416 total), representing 95·2% of the possible data out to a resolution of 1·83 Å. The data are 98·9% complete out to a resolution of 1·91 Å, and 80·7% complete in the 1·91-1·83 Å shell. The value of R_{symm} is 5·21% for all data.

(b) *Structure determination and refinement*

The general refinement strategy employed in the refinement of the deoxyβ_4 structure was described by Borgstahl *et al.* (1993). The starting atomic co-ordinates used for the refinement of the deoxyβ_4 structure were taken from the initial 2·5 Å COβ_4 atomic model. These co-ordinates were refined with the program PROLSQ against an initial 2·5 Å deoxyβ_4 dataset to an R-value of 22·7%. Four sulfate and 57 water molecules were added and the model was further TNT refined to an R-value of 18·2%. At this point, new crystals were grown and the 1·83 Å data collected. Cycles of manual rebuilding (including adjustments to the water structure) followed by TNT refinement reduced the R-value to 21·9%. Final cycles of refinement were carried out with PROLSQ and included the modeling of amino acids with dual conformations.

The final 1·9 Å model of deoxyβ_4, which consists of 4630 non-hydrogen protein atoms, 4 deoxy-heme groups, 68 water molecules and 4 sulfate ions, has an R-value of 19·0%. The final r.m.s. deviation from ideal geometry was 0·013 Å for bond lengths and 0·033 Å for bond angle distances. The average temperature factor of the whole model is 32·8 Å^2 and 32·1 Å^2 for the protein alone. The average water temperature factor is 44·2 Å^2 ($\sigma = 9{\cdot}0$) with a minimum of 26·1 Å^2 and a maximum of 58·9 Å^2. In the final stages of the refinement of the deoxyβ_4 atomic model, 36 residues were modeled with dual conformations (Table 1).

(c) *Construction of a T state β_4 model*

A hypothetical T state model of deoxyβ_4 was constructed by replacing the α1, α2, β1 and β2 subunits of human deoxyHb (Kavanaugh *et al.*, 1992*a*) with the corresponding β subunits from the refined structure of deoxyβ_4. Least-squares superpositions were carried out by including only the main-chain atoms of residues at the $\alpha1\beta2$ interface in the calculations (residues C2-CD2, F9-G4 and HC2; r.m.s. deviations 0.93 Å (α1 onto β1), 0·99 Å, (α2 onto β2), 0·42 Å (β1 onto β4) and 0·49 Å (β2 onto β3).

3. Results and Discussion

(a) *Characterization of the quaternary structure of deoxyβ_4*

(i) *Comparison of the quaternary structures of COβ_4 and deoxyβ_4*

The quaternary structure of the β_4 tetramer changes very little upon ligation. Since residues with dual conformations should be fairly sensitive to changes in local protein environment, the fact that interface residues Arg40(C6), Asp99(G1) and Cys112(G14) have dual conformations in both COβ_4 and deoxyβ_4 shows how similar the interfaces are (Table 1). In addition, the interface close contacts of deoxyβ_4 (not shown) are nearly identical with those listed for COβ_4.

In order to study the small differences in quaternary structure between COβ_4 and deoxyβ_4, one subunit of the COβ_4 tetramer was superimposed onto the corresponding subunit of deoxyβ_4, and then viewed as shown in Figure 1 for the interface

Table 1
Deoxyβ_4 residues with dual conformations

β1		β2		β3		β4	
...		—		Glu6(A3)	S	Glu6(A3)	S, L
		Leu14(A11)	B	—		—	
—		Lys17(A14)	I	—		—	
—		—		—		Glu26(B8)	S
Arg40(C6)	I	Arg40(C6)	I	Arg40(C6)	I	Arg40(C6)	I
—		—		—		Glu43(CD3)	S
Phe71(E15)	B	Phe71(E15)	B	Phe71(E15)	B	Phe71(E15)	B
Asp73(E17)	S	—		Asp73(E17)	S, L	—	
—		Leu75(E19)	B	—		—	
—		—		Lys82(EF6)	S	Lys82(EF6)	S
Asp99(G1)	I	Asp99(G1)	I	Asp99(G1)	I	Asp99(G1)	I
Cys112(G14)	I	Cys112(G14)	I	Cys112(G14)	I	Cys112(G14)	I
His117(G19)	S	His117(G19)	S	—		His117(G19)	S
Glu121(GH4)	S, L	—		Glu121(GH4)	S	—	
Lys132(H10)	S	Lys132(H10)	S	Lys132(H10)	S	Lys132(H10)	S

The residue environment is indicated by S (surface residue), L (lattice contact), B (buried side-chain) and I (subunit-subunit interface)

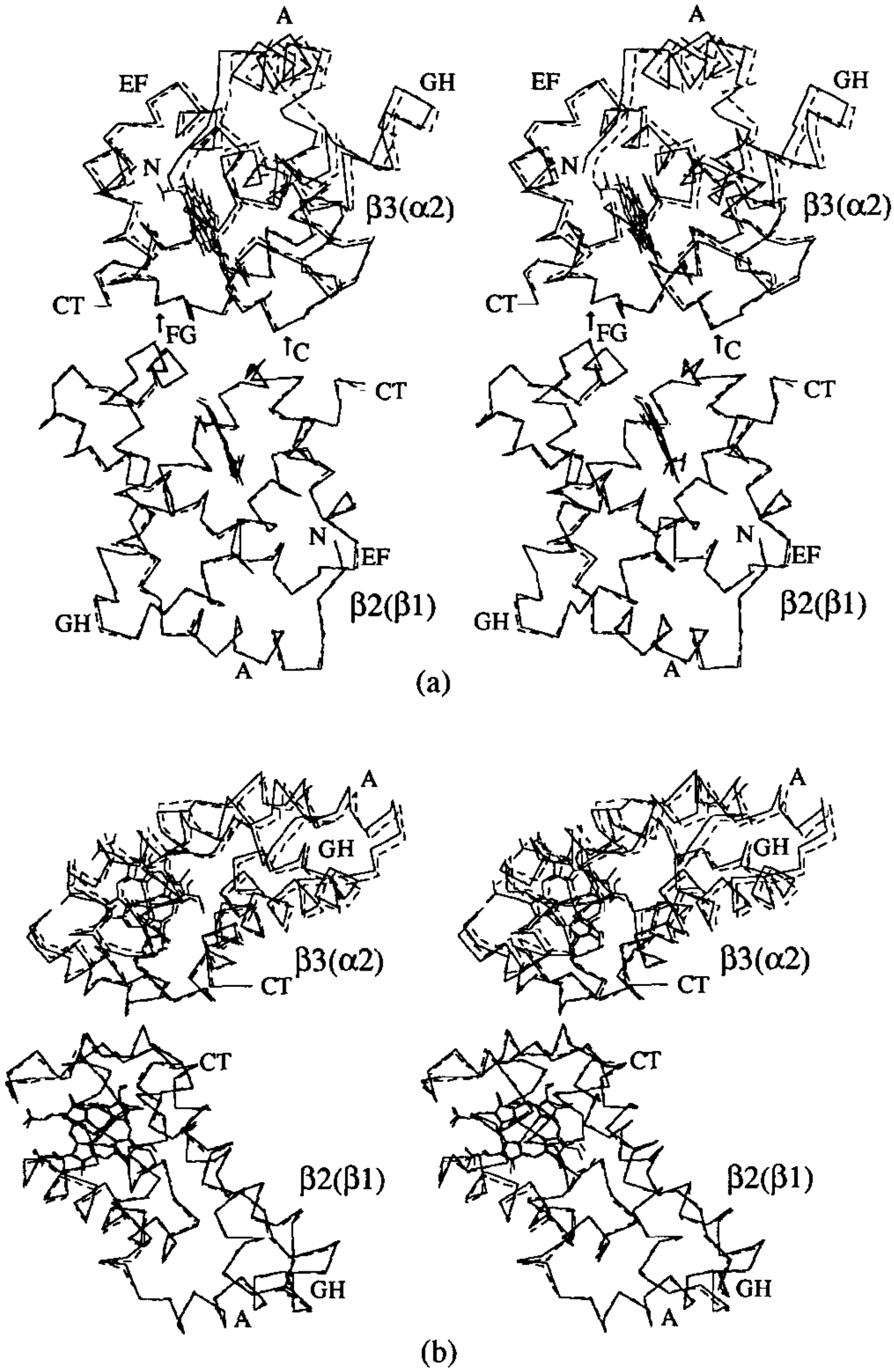

Figure 1. Stereo drawings of C^{α} tracings comparing the $\beta2\beta3(\alpha2\beta1)$ subunit-subunit interfaces of deoxyβ_4 (continuous line) and COβ_4 (broken line); (a) front and (b) side views. The main-chain atoms (residues 1 to 19, 22 to 42, 45 to 145) of the $\beta2$ subunit (bottom subunit) from COβ_4 and deoxyβ_4 were superimposed (r.m.s. deviation = 0·29 Å).

that corresponds to the $\alpha1\beta2$ interface of the $\alpha_2\beta_2$ tetramer. Both orthogonal views of this interface show that the nonsuperimposed COβ_4 subunit is rotated relative to the same deoxyβ_4 subunit about an axis that passes through the $\beta2\beta3$ interface. This rotation produces maximal deviations in structure (~1·5 Å) at the A helix, EF corner and GH corner, and minimal deviations (~0·4 Å) at the C helix and FG corner. Since the minimal C^{α} deviations are about twice as large as the corresponding differences of the superimposed subunits (data not shown), it appears that the COβ_4 interface may be spread apart very slightly (~0·1 Å) on average relative to the deoxyβ_4 interface. Similar analysis of the other

β_4 interfaces shows that a very small ligand-induced rotation also takes place about the $\beta2\beta4(\beta1\beta2)$ interface, but there is no significant change at the $\beta1\beta2(\alpha1\beta1)$ interface (figures not shown). Thus, a small ligand-induced rotation of the $\beta1\beta2(\alpha1\beta1)$ dimer relative to the $\beta3\beta4(\alpha2\beta2)$ dimer appears to take place in the β_4 tetramer. However, these changes are an order of magnitude smaller than the quaternary structure changes associated with co-operative ligand binding in the $\alpha_2\beta_2$ tetramer, and ligand binding to β_4 does not result in a change in the interdigitation pattern of the $\beta1\beta4(\alpha1\beta2)$ subunit interface. Clearly, the non-cooperative β_4 tetramer is frozen in a quaternary structure that very closely resembles the R state of $\alpha_2\beta_2$.

The lack of a large change in quaternary structure is consistent with the β_4 tetramer's very low level of heterotropic allosterism (Benesch & Benesch, 1974; Kurtz *et al.*, 1981). Since deoxy and liganded β_4 both have an R-like quaternary structure, the residues responsible for the alkaline Bohr effect, for example, do not alter their environments significantly, and therefore their pK values should remain unchanged. His146β, in particular, is responsible for about 40% of the alkaline Bohr effect at physiological salt concentrations in human Hb because its imidazole side-chain forms a strong salt bridge with Asp94β in deoxyHb, but not in the R state of liganded Hb, where it is highly solvated (Perutz, 1970; Kilmartin, 1977). In the β_4 tetramer, the side-chain of His146β interacts only weakly with the surrounding protein in both the deoxy and fully liganded forms, and therefore there is no structural reason for its degree of protonation to be strongly linked to oxygen binding.

(ii) *Analysis of a hypothetical T state β_4 tetramer*

On the basis of symmetry arguments alone, Dickerson & Geis (1983) have reasoned that β_4 should not be stable as a T state tetramer. They pointed out that the R state $\alpha_2\beta_2$ tetramer is more symmetric than the T state because the homologous joint and switch regions of the $\alpha1\beta2$ interface have the same interdigitation pattern in the R state, but not in the T state. Therefore, it is seems reasonable to expect a homotetramer like β_4 to adopt the more symmetric R state quaternary structure. However, we find that both liganded and deoxyβ_4 do not display exact 222 symmetry. In order to form the stabilizing Arg40···Asp99 salt-bridge across the $\beta1\beta4(\alpha1\beta2)$ interface, steric constraints dictate that this β_4 interface must be asymmetric. It is conceivable, therefore, that β_4 could form the more asymmetric T state tetramer as a way of preventing destabilizing steric conflicts imposed by the symmetry of the R state, or as a way of forming asymmetric stabilizing interactions between the hinge and switch regions.

We have examined a hypothetical model of a T state β_4 molecule in order to determine if stereochemical conflicts prevent the formation of a stable T state $\beta1\beta4(\alpha1\beta2)$ interface. Inspection of this model shows that when the switch region has a T state interdigitation pattern (where His97(FG4)β4 lies between Arg40(C6)β1 and Glu43(CD2)β1) Arg40 is thrust so deeply into the center of the interface that it is too close to Asp99 to form a stable ionic interaction (Fig. 2). This steric conflict could not be relieved by manually adjusting the torsion angles of Arg40 and Asp99 to alternative conformations. Moreover, the alternative conformation of Arg40 (shown as Arg40(C6)β4 in Fig. 2) that is observed in the R state β_4 quaternary structure cannot occur in the T state because steric conflicts develop with the main-chain atoms of residues His97 and Val98. Thus, a T state $\beta1\beta4(\alpha1\beta2)$ interface simply does not have enough room to accommodate an arginine residue at position C6.

Forming a T state switch interdigitation pattern also results in an increase in exposed hydrophobic surface. In particular, Trp37(C3) is more accessible to solvent in the T state β_4 model than it is in the deoxyβ_4 crystal structure. Solvent-accessible surface areas, calculated using the CHARMm/QUANTA software (Polygen Corp., Waltham, MA), indicate that 25·3 Å^2 of Trp37 becomes exposed in a hypothetical R-to-T transition. The accessible surface area of Trp37 is 42·8 Å^2 in the T state model *versus* 17·5 Å^2 in the deoxyβ_4 crystal structure because side-chain atoms CZ2, CZ3 and CH2 are more accessible to water. Similar calculations with the $\alpha_2\beta_2$ tetramer show that the R-to-T transition also show an increase of 23·6 Å^2 of accessible surface area for Thr38(C3)α. However, the transfer of a threonine side-chain to the protein surface is energetically more favorable than the corresponding transfer of a tryptophan side-chain. According to Janin and co-workers (Janin *et al.*, 1988), the surface/interior transfer free energy (a free energy that reflects the frequency with which a given amino acid type partitions between the protein interior and its surface) is −0·19 kcal/mol for threonine and 0·28 kcal/mol for tryptophan. Therefore, increased exposure of residue C3 favors the R-to-T transition in the $\alpha_2\beta_2$ tetramer and inhibits it in the β_4 tetramer.

Another factor that militates against the stabilization of a T state β_4 tetramer is the inability of the COOH-terminal carboxyl groups to form intersubunit salt bridges (not shown), interactions that have been proposed to stabilize the $\alpha_2\beta_2$ T state (Perutz, 1970). In T state $\alpha_2\beta_2$ tetramers, the carboxyl group of His146(HC3)β forms a strong ionic contact with the ε-amino group of Lys40(C5)α across the $\alpha1\beta2$ interface. However, in the β_4 tetramer Lys40(C5)α is replaced by Gln39(C5)β. This substitution eliminates the possibility of an intersubunit salt bridge, and even a hydrogen bond is unlikely because the side-chain at position C5 is shortened by one covalent bond.

(b) *Characterization of the tertiary structure of deoxyβ_4*

There are two known quaternary structures for liganded human Hb, and these structures were compared with COβ_4 in the accompanying paper

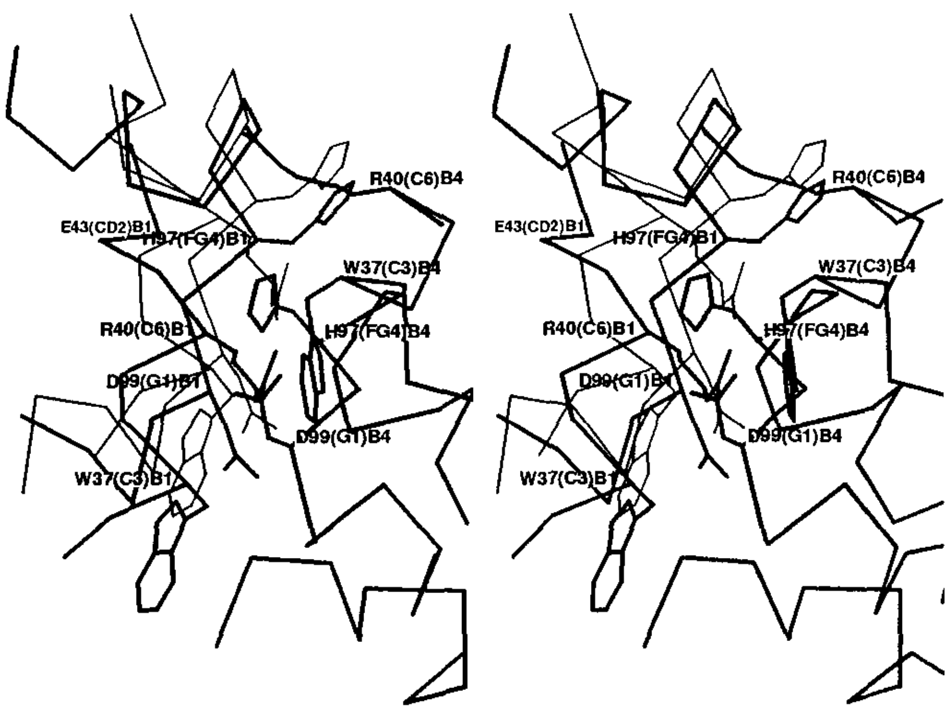

Figure 2. Stereo drawing of C^{α} tracings comparing the $\beta1\beta4(\alpha1\beta2)$ interfaces of deoxyβ_4 (thin line) and a hypothetical T-state deoxyβ_4 model (bold line). Side-chains of residues Trp37(C3), Arg40(C6), His97(FG4) and Asp99(G1) are shown. The $\beta4$ subunits were superimposed. Only single conformers of Arg40 and Asp99 are represented with Arg40$\beta1\cdots$Asp99$\beta4$ forming the intersubunit salt bridge and Arg40$\beta4\cdots$Asp99$\beta1$ pointing out of the interface.

(Borgstahl *et al.*, 1993). The R-state structure of human oxyHb (oxyHb(R)) was determined at 2·1 Å resolution with crystals grown from high-salt solutions (Shaanan, 1983), and the R2 state structure of COHb (COHb(R2)) was determined at 1·7 Å resolution with crystals grown from relatively low-salt solutions (Silva *et al.*, 1992). There is only one known quaternary structure for deoxyHb, the T-state (deoxyHb(T)) and it has been determined under high-salt conditions at 1·7 Å (Fermi *et al.*, 1984) and 1·5 Å resolution (Kavanaugh *et al.*, 1992*a*), as well as under low salt conditions at 1·9 Å resolution (Kavanaugh *et al.*, 1992*b*). By comparing these structures with those of COβ_4 and deoxyβ_4 the ligand-induced changes in tertiary structure can be separated from those that are solely due to a change in quaternary structure.

(i) *Heme stereochemistry*

Heme stereochemistry is critically linked to Hb function. It is now well known that the transition from the unliganded T state to the liganded R state results in a movement of the heme iron into the plane of the porphyrin nitrogen atoms, a flattening of the porphyrin pyrrole ring system, and the shortening of the proximal histidine–iron bond (Perutz, 1979). The influence of protein structure alone on heme stereochemistry is not understood as well due to a lack of high-resolution crystal structures that can be used to partition the effects of ligand binding from the effects due to changes in protein structure. The refined structures of COβ_4, deoxyβ_4, and deoxyHb constitute a set of structures that can be used to carry out such a partitioning.

The refinement of most protein structures requires the use of restraints on both the covalent and non-covalent interactions in order to maintain valid stereochemistry, and the type and strength of these restraints can significantly affect the final geometry of the refined model. In particular, this is true for heme geometry, and it has been demonstrated for several 2·1 Å Hb structures that various refinement programs and protocols can produce significantly different results (Liddington *et al.*, 1992). In order to minimize this kind of experimental problem, the Hendrickson-Konnert refinement program was used in a consistent manner for the final refinement cycles of all Hb structures reported in this paper. Specifically, the COHb(R2) and COβ_4(R) carbonmonoxy hemes as well as the deoxyHb(T) and deoxyβ_4(R) unliganded hemes were refined against idealized porphyrins with planar restraints applied to each of the four pyrrole rings (but not to the entire porphyrin). In addition, for each Hb structure "special distances" between the proximal histidine (His F8) and the heme (i.e. the Fe-$N^{\varepsilon2}$ bond length as well as the Fe-$C^{\varepsilon1}$, Fe-$C^{\delta2}$ and the four $N^{\varepsilon2}$-porphyrin N non-covalent distances) were weakly restrained ($\sigma = 0·1$ Å) with His F8 oriented symmetrically with respect to the heme group.

A set of parameters that define heme stereochemistry is presented in Table 2 for the liganded $\alpha_2\beta_2$ tetramers (COHb(R2) and oxyHb(R)), COβ_4(R) and deoxyβ_4(R), the T state of deoxy $\alpha_2\beta_2$, and BME-deoxyHb(R). The 1·8 Å BME-deoxyHb(R) crystal structure was determined with crystals of aquometHb that were first reacted with bis(N-maleimidomethyl) ether (BME), a bifunctional reagent that cross-links Cys93(F9) to His97(FG4) in the same β subunit, and then reduced with dithionite (Perutz, 1970; Perutz *et al.*, 1987). This covalent cross-link locks Hb in the R quaternary structure so that reduction to the deoxy state does not crack or disorder the crystals. Therefore, like deoxyβ_4, BME-deoxyHb is a model for deoxyHb in the R state.

The distance from the heme iron to the plane of the porphyrin nitrogen atoms, Fe-P$_N$ in Table 2, and the Fe-N$_{porph}$ bond lengths are key parameters of heme-iron stereochemistry (Perutz, 1979). In low-spin six-co-ordinate iron porphyrins, the heme is essentially flat, and the iron is in (or very near) the heme plane. In high-spin five-co-ordinate iron porphyrins, the change in co-ordination and spin state result in a lengthening of the Fe-N$_{porph}$ bonds, displacement of the iron from the plane of the porphyrin nitrogen atoms, and a slight dome shape to the heme group. The data in Table 2 show that the heme iron is in the plane of the porphyrin nitrogen atoms for COHb(R2) and COβ_4(R), while it is slightly below (i.e. on the distal side) the plane for oxyHb(R). This may be a real difference, or it may simply be due to differences in the quality of the diffraction data and refinement methods. In all three liganded structures, the Fe-N$_{porph}$ bonds have (within the accuracy of the measurements) the same value of $\sim$1·99 Å. In the deoxyHb(T), the iron is 0·33 Å out of the plane of the porphyrin nitrogen atoms and the Fe-N$_{porph}$ bond lengths increase to 2·06 Å. Essentially the same values are observed for deoxyβ_4. Therefore, a change in quaternary structure from the T state of the $\alpha_2\beta_2$ tetramer to the R state structure of deoxyβ_4 does not have a measurable impact on the iron stereochemistry of the β subunit heme groups. Comparison of the β heme groups of R state BME-deoxyHb with those of T state deoxyHb leads to the same conclusion if one assumes that the small difference in Fe-P$_N$ is due to experimental error or to an effect of the chemical cross-link.

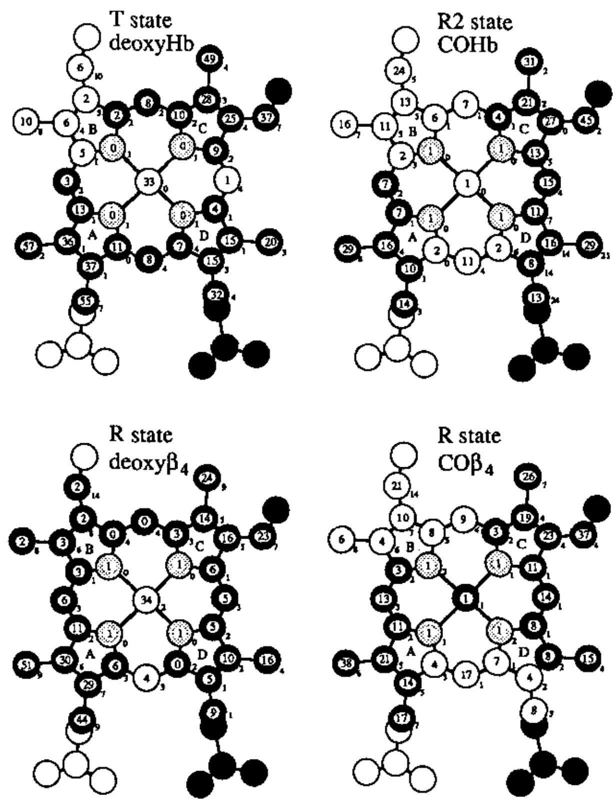

Figure 3. Heme topology diagrams. A least-squares plane, P$_N$, through the 4 heme nitrogen atoms (gray circles) was calculated and then the distance of each atom above (white circles) or below (black circles) P$_N$ is given in hundredths of an ångström unit. The standard deviation of the mean is indicated to the lower right of each average.

Table 2
Heme stereochemistry of β subunits in various hemoglobins

	R2 state COHb	R state oxyHb	R state COβ_4	R state deoxyβ_4	T state deoxyHb	R state BME-deoxyHb
Distances (Å)†						
Fe-P$_N$	−0·01 (0)	0·11	0·01 (1)	−0·34 (2)	−0·33 (0)	−0·27
Fe-N$_{porph}$	1·99 (1)	1·96 (6)	2·02 (2)	2·06 (1)	2·06 (4)	2·07 (3)
Fe-His(F8)N$^{\varepsilon 2}$	2·10 (0)	2·07	2·10 (2)	2·15 (2)	2·22 (2)	2·14 (4)
NC-His(F8)C$^{\delta 2}$	3·06 (1)	3·1	3·12 (4)	3·60 (5)	3·79 (0)	–
NA-His(F8)C$^{\varepsilon 1}$	3·05 (2)	3·0	2·97 (3)	3·19 (3)	3·21 (3)	—
Prox. His(F8) angles (deg.)‡						
Roll	12 (2)	27	16 (2)	19 (2)	22 (2)	–
Pitch	2 (1)	5	3 (1)	2 (1)	2 (1)	—
Yaw	2 (1)	4	2 (1)	5 (1)	9 (1)	

Average in Å (standard deviation of the mean × 100). Negative distances are towards the proximal side. Average angles in degrees (standard deviation of the mean). The oxyHb(R) structure Protein Databank entry 1HHO) was refined with the Jack-Levitt procedure (Jack & Levitt, 1978). Refinement details of BME-deoxyHb(R) were not reported (Perutz *et al.*, 1987).

†P$_N$ least-squares plane calculated with porphyrin nitrogen atoms only (4 atoms). N$_{porph}$: porphyrin N-Fe distances.

‡*Roll*, angle between His normal and NA-NC line −90°. *Pitch*, angle between P$_N$ and His plane −90°. *Yaw*, angle between HisN$^{\varepsilon 2}$-Fe bond and P$_N$ normal.

An analysis of the heme planarity for β subunits of the high-resolution structures of COβ_4(R), deoxyβ_4(R), COHb(R2) and deoxyHb(T) is presented in Figure 3. Comparison of the COHb(R2) and COβ_4(R) β heme diagrams reveals that in both tetramers the pyrrole rings A, C and D are below the plane of the four heme nitrogen atoms, P_N, by about the same magnitude and pyrrole ring B is above P_N by the same magnitude. Likewise, the β heme diagrams of deoxyHb(T) and R state deoxyβ_4 show that in these tetramers pyrrole rings A, C and D are below the P_N plane and the plane of pyrrole ring B is not significantly different from P_N. Ring C (and ring D to some extent) is slightly further below P_N in deoxyHb(T) than in R state deoxyβ_4. This appears to be correlated with the position of the FG corner relative to the heme (see Fig. 5). It is clear, however, that pyrrole ring A deviates from the P_N plane significantly more in deoxyHb(T) and deoxyβ_4(R) than in the COHb(R2) and COβ_4(R) structures. Overall heme topology appears to be mainly a function of heme ligation state and is not as greatly influenced by tetramer quaternary structure.

Other parameters listed in Table 2 are a measure of the stereochemical relationship between the proximal histidine and the heme. Specifically, the NC···His(F8)$C^{\delta 2}$ and NA···His(F8)$C^{\varepsilon 1}$ non-covalent distances are nearly equal in COHb(R2), oxyHb(R) and COβ_4(R), with values of 3·0 Å to 3·1 Å, indicating that the proximal histidine adopts a symmetric orientation relative to the heme in these liganded structures. In contrast, the NC···His(F8)$C^{\delta 2}$ and NA···His(F8)$C^{\varepsilon 1}$ distances are 3·60 Å and 3·19 Å, respectively, in deoxyβ_4 and 3·79 Å and 3·21 Å in deoxyHb(T), reflecting an asymmetric proximal histidine–heme orientation in these unliganded structures (despite the weak symmetric restraints mentioned above). The degree of proximal histidine–heme asymmetry is significantly less, however, in deoxyβ_4(R) than in deoxyHb(T). Relative to deoxyHb(T), the NC···His (F8)$C^{\delta 2}$ distance is reduced by 0.19 Å and the angle between the Fe-His(F8)$N^{\varepsilon 2}$ bond and the P_N plane normal (the yaw angle in Table 2) is reduced from 9° to 4° in deoxyβ_4(R). Thus, it would appear that while ligation state controls the His(F8)-heme stereochemistry to a large extent, the R-to-T quaternary transition also contributes significantly to the proximal histidine–heme asymmetry in deoxyHb.

Finally, we address the question of the affect of changes in quaternary structure on the Fe-His(F8)$N^{\varepsilon 2}$ bond distance. The Fe-His(F8)$N^{\varepsilon 2}$ bond distances listed in Table 2 indicate that liganded β heme groups have values between 2·07 Å and 2·10 Å, and Philips (1980) reported a value of 2·07 Å for a 1·6 Å oxymyoglobin structure. For high-resolution deoxyHb(T) crystal structures, namely the 1·5 Å high-salt and the 1·9 Å low-salt structures, the β subunit Fe-His(F8)$N^{\varepsilon 2}$ bond ranges from 2·19 Å to 2·22 Å. Thus, ligand binding coupled with a T-to-R quaternary structure change results in a shortening of the Fe-His(F8)$N^{\varepsilon 2}$ bond from ~2·20 Å in deoxy T-state structures to ~2·09 Å in liganded R-state structures.

In all the PROLSQ refinements the Fe-His (F8)$N^{\varepsilon 2}$ bond was weakly restrained ($\sigma \geq 0{\cdot}1$ Å) to a length within ~0·005 Å of the final average refined value. For example, when the low-salt deoxyHb(T) structure was refined with a 2·10 Å restraint, the average value converged to 2·16 Å. Resetting the restraint to 2·16 Å resulted in a value of 2·18 Å, and when the restraint was finally set to 2·20 Å, an average value of 2·205 Å was obtained. In the case of the deoxyβ_4(R) tetramer, restraints of 2·10 Å, 2·15 Å and 2·20 Å, resulted in average values of the Fe-His(F8)$N^{\varepsilon 2}$ bond length of 2·12 Å, 2·15 Å and 2·18 Å, respectively, suggesting that 2·15 Å is the best estimate. These results infer that the deoxy T state β heme has a Fe-His(F8)$N^{\varepsilon 2}$ bond length of ~2·20 Å, whereas the unliganded R state β heme has a shorter value of 2·15 Å for deoxyβ_4 and 2·14 Å for BME-deoxyHb. That is, a change in quaternary structure alone from the deoxy T state to the R state of deoxyβ_4 or BME-deoxyHb appears to shorten the Fe-His(F8)$N^{\varepsilon 2}$ bond distance to a value about halfway between that of deoxy T state Hb and liganded R state Hb.

While the resolution of the diffraction data makes an accurate determination of the Fe-His(F8)$N^{\varepsilon 2}$ bond length difficult, the direction of the change is consistent with the R-to-T linked change of the Fe-His(F8)$N^{\varepsilon 2}$ bond stretching frequency ($\nu_{Fe\text{-}His}$) as determined by resonance Raman spectroscopy (Nagai & Kitagawa, 1980). Moreover, Kitagawa (1992) correlated $\nu_{Fe\text{-}His}$ with the first Adair constant for deoxyHb A, several mutant deoxyHbs, and deoxyβ_4 over a wide range of conditions. Of all Hb studied, deoxyHb in the T state had the lowest $\nu_{Fe\text{-}His}$ and deoxyβ_4 had the highest $\nu_{Fe\text{-}His}$. Kitagawa (1992) concluded that the Fe-His(F8)$N^{\varepsilon 2}$ bond is stretched in the T state, and that the "strain on the Fe-His(F8)$N^{\varepsilon 2}$ bond imposed by the globin is evidently one of the important factors that control oxygen affinity".

(ii) *Quaternary and ligand-induced changes in β-chain tertiary structure*

The changes in structure that occur as a result of the transition from the unliganded T state to the liganded R state have been analyzed in great detail (e.g., see Perutz, 1970; Baldwin & Chothia, 1979; Gelin *et al.*, 1983, Perutz *et al.*, 1987) and in Figure 4 the β heme environment in oxyHb(R) is compared with deoxyHb(T) by superimposing the heme groups. On the proximal side of the heme the structural change has been dissected into four major movements: (1) the heme iron moves into the plane of the porphyrin nitrogen atoms, (2) the heme group rotates about an axis passing through pyrrole rings B and D, (3) the heme-linked proximal His(F8) shifts toward the heme and assumes a more symmetric position relative to the heme (Fig. 4(a)), and (4) the F helix moves toward the $\alpha1\beta2$ interface and the FG corner, which is part of the $\alpha1\beta2$ interface switch region, moves parallel to the $\alpha1\beta2$ inter-

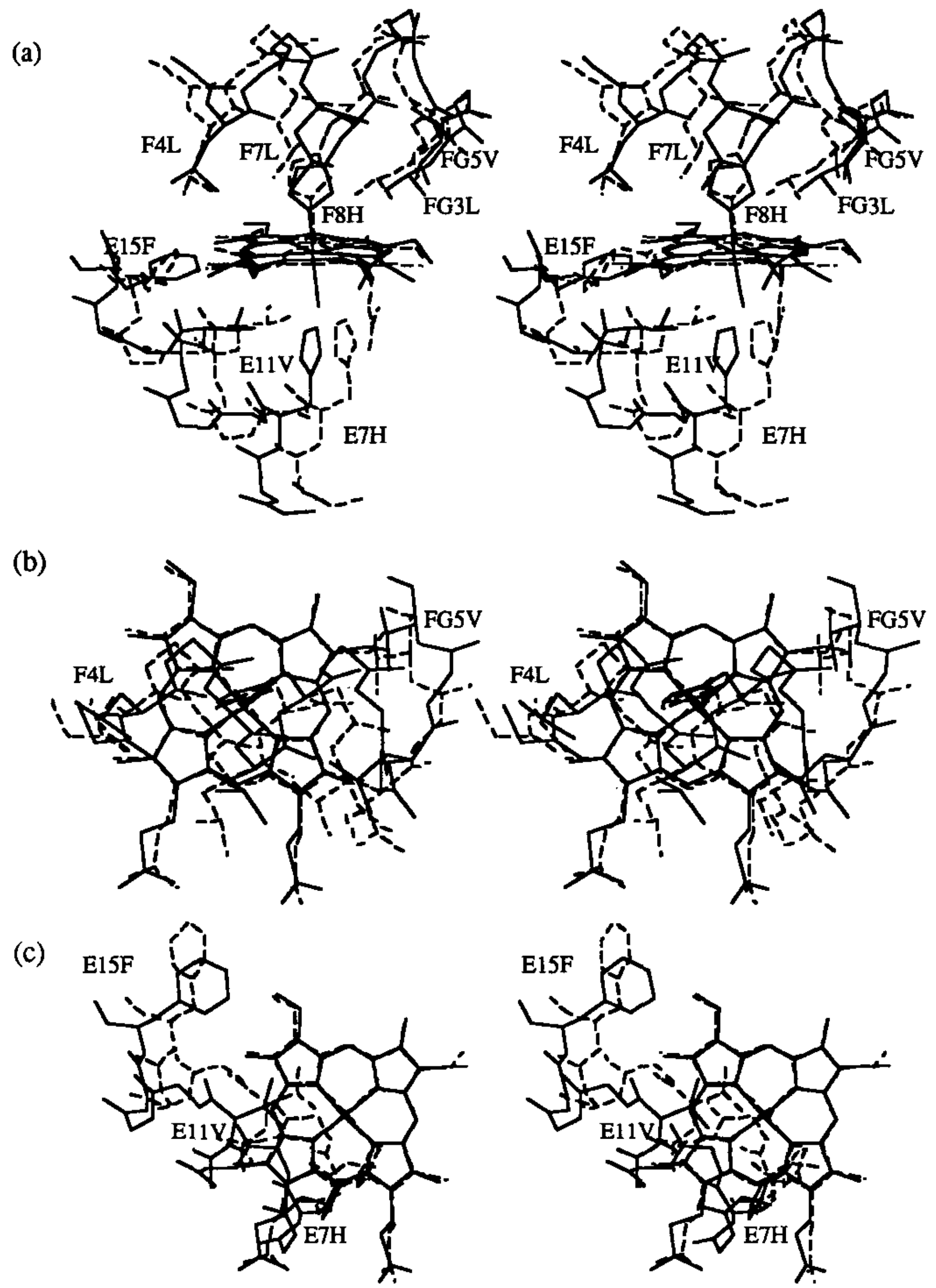

Figure 4. Tertiary structure changes relative to the heme group for the transition from oxyHb(R) (continuous lines) to deoxyHb(T) (broken lines); (a) E helix, F helix and FG corner, side view; (b) F helix and FG corner, top view; (c) E helix, top view. Selected side-chains of residues facing the heme are shown. The heme groups of oxyHb(R) and deoxyHb(T) were superimposed using 12 porphyrin atoms (NA, CA1, CA4, NB, CB1, CB4, NC, CC1, CC4, ND, CD1 and CD4; r.m.s. deviation = 0·13 Å).

face (Fig. 4(b)). On the distal side of the heme, the E helix shifts relative to the heme providing room for the bound ligand (Fig. 4(c)). The F helix shifts 1·0 Å, the E helix shifts 1·9 Å, and the β FG corner moves 1·6 Å, relative to the heme.

By analyzing the structural differences between deoxyHb(T) and deoxyβ_4(R) in Figure 5, the changes in β subunit tertiary structure due solely to the quaternary structure transition between the deoxy T state and the deoxy R state can be isolated from those due to ligand binding. Likewise, by analyzing the structural differences between deoxyβ_4(R) and COβ_4(R) in Figure 6, the changes in β subunit tertiary structure due solely to ligand binding can be partitioned from those due to changes in quaternary structure. Relative to the

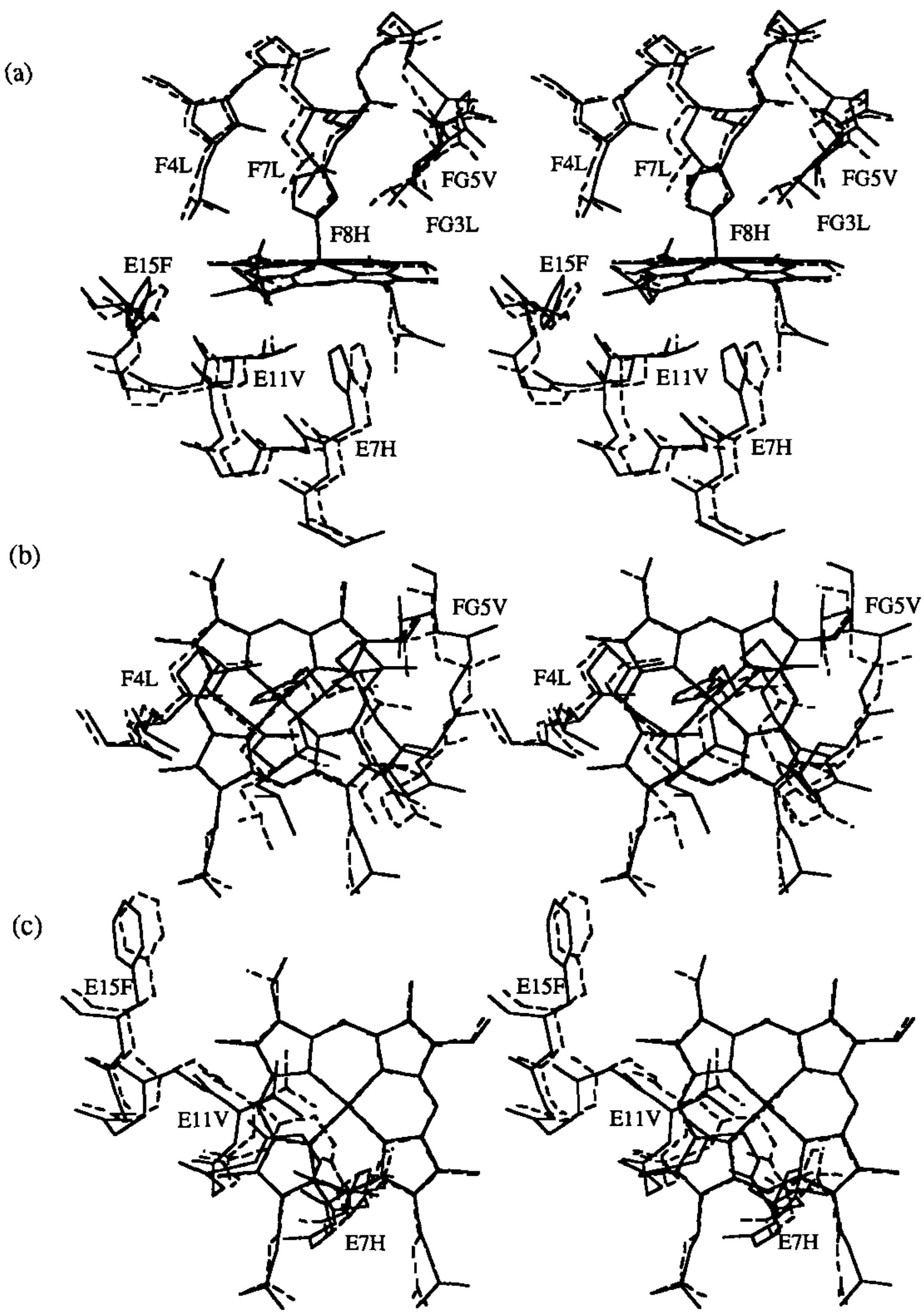

Figure 5. Quaternary-induced changes in tertiary structure relative to the heme group for the transition from deoxyHb(T) (broken lines) to the R state deoxyβ_4 (continuous lines); (a) E helix, F helix and FG corner, side view; (b) F helix and FG corner, top view; (c) E helix, top view (r.m.s. deviation = 0·06 Å).

heme group the deoxy T to deoxy R quaternary structure change (Fig. 5) results in shifts of the F helix, FG corner and E helix that have the same directional components, but with reduced magnitudes, as those observed in the full deoxy T to liganded R transition (Fig. 4). Specifically, the β F helix moves about 0·6 Å in the direction of the $\alpha1\beta2$ interface (Fig. 5(a) and (b)), the β FG corner shifts about 1·1 Å parallel to the $\alpha1\beta2$ interface, and the E helix shifts by about 0·9 Å away from the heme to open the heme pocket (Fig. 5(a) and (c)). Figure 6 shows that the binding of ligand to R state deoxyβ_4

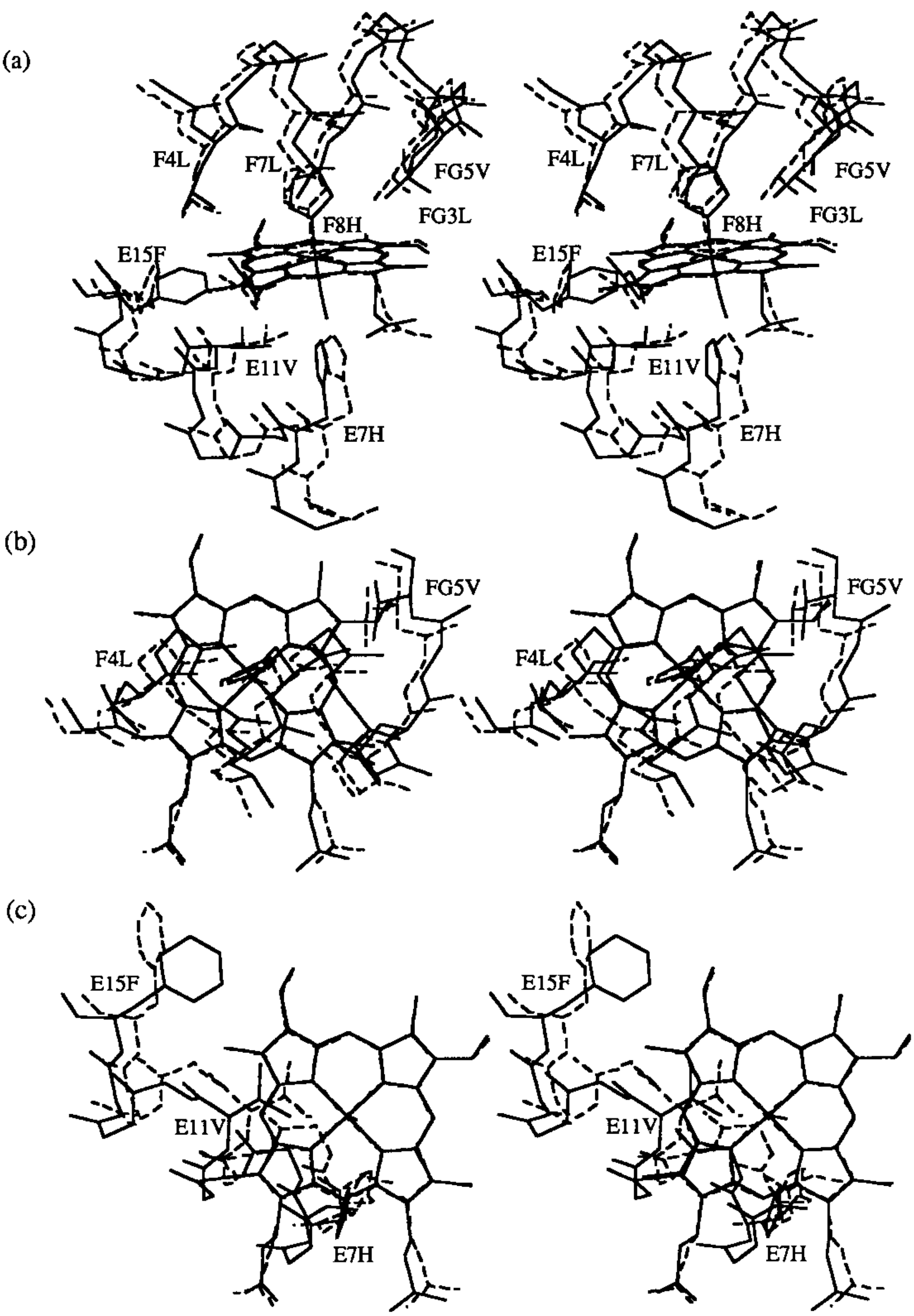

Figure 6. Ligand-induced changes in tertiary structure relative to the heme group for the transition from R state deoxyβ_4 (broken lines) to R state COβ_4 (continuous lines); (a) E helix, F helix and FG corner, side view; (b) F helix and FG corner, top view; (c) E helix, top view (r.m.s. deviation = 0·06 Å).

induces the other half of the movements of the F helix (~0·6 Å), FG corner (~0·7 Å), and the E helix (~1·0 Å).

While not shown in Figure 6, Val98(FG5) is observed to have two conformations in COβ_4(R) (Table 1 in Borgstahl *et al.* 1993), but only one conformation in deoxyβ_4(R). In this case, a small change in the packing interactions between the side-chain of Val98(FG5) and the heme shifts the rotamer equilibrium such that the dominant conformation in COβ_4(R) is the only conformation observed in deoxyβ_4(R). In the case of Phe71(E15),

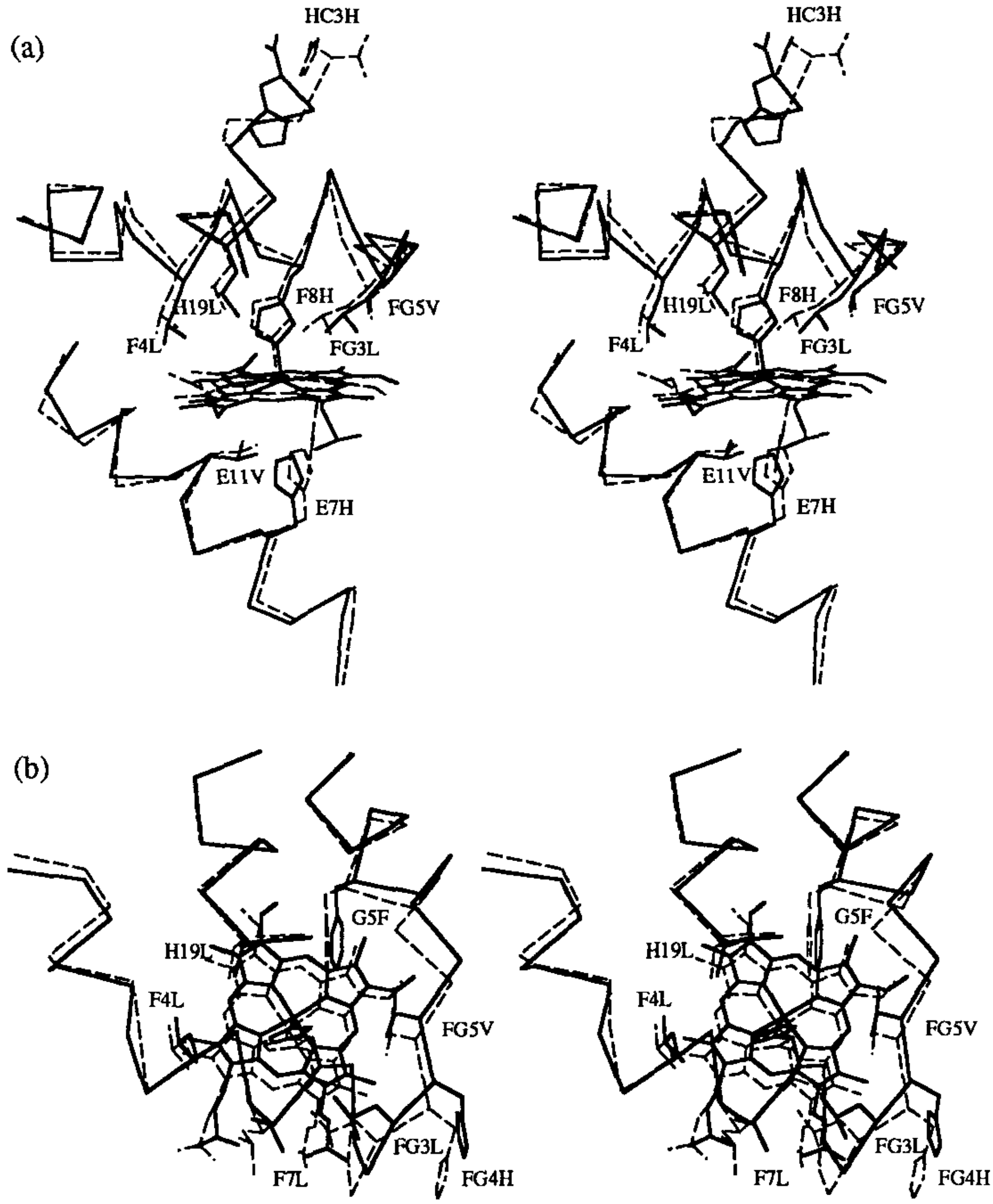

Figure 7. The quaternary-induced changes in tertiary structure for the E helix, F helix, FG corner, H helix and COOH-terminal peptide relative to the β subunit main-chain atoms for the transition from deoxyHb(T) (broken lines) to R state deoxyβ_4 (continuous lines); (a) front view, (b) top view. The main-chain of residues 14 to 20, 23 to 40, 48 to 74, 77 to 90, 102 to 116 and 122 to 140 were included in the least-squares superposition (r.m.s. deviation = 0·52 Å).

two conformations are observed in both COβ_4(R) and deoxyβ_4(R), but the roles of the dominant and minor rotamers are reversed in the two structures.

In Figure 7, the backbone atoms of a β subunit of deoxyβ_4(R) have been superimposed onto a β subunit of deoxyHb(T). Changing the frame of reference from the β heme group to the β subunit backbone reveals more clearly how the quaternary transition from the deoxy T state to the deoxy R state transition alters β subunit tertiary structure. In deoxyHb(T), His97(FG4)β2 is positioned between Thr41(C6)α1 and Pro44(CD2)α1. This is the switch region of the α1β2 interface, and transition to the R state requires that His97(FG4)β2 "jump" a turn of the α1 C helix so that it is repositioned between Thr41(C6)α1 and Thr38(C3)α1. The superposition in Figure 7 shows that this change in quaternary structure is directly coupled to a change in β-chain tertiary structure, a shift of the end of the F helix, the FG corner, and the beginning of the G helix (residues Leu91(F7) through Phe103(G5)). This structural unit of the β-chain is essentially equivalent to the "allosteric core" identified by Gelin *et al.* (1983) through the use of energy minimization calculations. The β heme group moves along with the allosteric core, since it is covalently attached to it, and forms non-covalent interactions with Leu88(F4), Leu91(F7), Leu96(FG3), Val98(FG5) and Phe103(G5). The T-to-R quaternary-induced movement of the allosteric core shifts the heme group by about 0·5 Å relative to the E helix to open up the ligand binding site. Relative to the deoxyHb heme group, the deoxyβ_4 heme rotates by 4·5° in response to the T-to-R change in quaternary structure. However, as the analysis in the heme reference frame showed, the heme group and the allosteric core do not move as a rigid body. The heme shifts its position relative to residues of the F helix and FG corner so that it adopts a more symmetric position relative to the proximal His(F8).

The β subunit COOH-terminal peptide and the end of the H helix are also shown in Figure 7(a). In deoxy $\alpha_2\beta_2$ Hb, the COOH-terminal residue, His146(HC3), forms two salt bridges (not shown): one is an intrasubunit interaction between its imidazole side-chain and the carboxyl group of Asp94(FG1), and the other is an intersubunit interaction between the COOH-terminal carboxyl group and Lys40(C5)α across the $\alpha1\beta2$ interface. Since the end of the H helix and the COOH-terminal peptide make several non-covalent interactions with the F helix, the His146 ··· Lys40 salt bridge acts an intersubunit strap that may inhibit small ligand-induced movements of the F helix in the T quaternary state. In deoxyβ_4, the intersubunit salt bridge cannot form because residue C5 is now glutamine, and the quaternary-induced T-to-R shift of the allosteric core includes a movement of Asp94(FG1) that ruptures the intrasubunit salt bridge in the R state.

4. Conclusion

The β subunits of the deoxyβ_4 tetramer have an affinity for oxygen that is over 200 times greater than the same β subunits of the deoxy $\alpha_2\beta_2$ tetramer (Imai, 1979). The structural basis for this increase in ligand affinity is that the change in quaternary structure from T state deoxy $\alpha_2\beta_2$ to R state deoxyβ_4 shifts the tertiary structure of the β subunits halfway toward the tertiary structure observed in liganded β_4 or liganded $\alpha_2\beta_2$. One aspect of this quaternary-induced change in tertiary structure is that the stereochemical relationship between the proximal His and the β heme group approaches the stereochemistry observed in liganded R state tetramers (Fig. 5(a)). Specifically, the Fe-His (F8)$N^{\varepsilon2}$ bond length is reduced by a few hundredths of an ångström unit, and the imidazole side-chain of His(F8) assumes a more symmetric orientation relative to the heme (Table 2). While the exact magnitude of the change in the Fe-His(F8)$N^{\varepsilon2}$ bond length in not certain at present, a small reduction should lead to a significant increase in oxygen affinity. Similarly, the theoretical calculations of Gelin & Karplus (1977) indicate that the more symmetric orientation His(F8) in deoxyβ_4(R) should result in an increase in ligand affinity because it would lead to less ligand-induced strain relative to the amount that develops in T state tetramers.

Another aspect of the quaternary-induced change in β subunit tertiary structure is a shift in the F helix, FG corner, G helix and the β heme group (the allosteric core) away from the E helix. This shift of the allosteric core has two structural consequences that should result in an increase in ligand affinity. First it opens up the ligand binding pocket. Perutz (1970) first noted that the position of Val67(E11) sterically inhibits ligand binding in the β subunits of deoxyHb. This steric block is greatly reduced in deoxyβ_4 (Fig. 5(b)). Secondly, the shift of the allosteric core may also release constraints between the F helix and the COOH-terminal peptide that tend to inhibit ligand-induced movements of the F helix (Fig. 7). Together, these co-ordinated effects work in unison to give deoxyβ_4 a tertiary structure that has high affinity for ligand.

The three-dimensional structures of the doubly and triply liganded intermediate Hb species with R-like quaternary structures are unknown. However, insights derived from the deoxyβ_4 Hb structure may be applicable to these intermediates because they have functional properties similar to those of the β_4 tetramer. In particular, the third and fourth ligands bind to doubly and triply liganded Hb with increasingly high affinity, and they exhibit quaternary enhancement (Ackers *et al.*, 1992; Mills & Ackers, 1979). (Quaternary enhancement refers to the phenomenon whereby the assembly of globin subunits into tetramers results in an increase in oxygen affinity.) Likewise, the β_4 tetramer has high ligand affinity (Benesch & Benesch, 1974), and exhibits quaternary enhancement (Valdes & Ackers, 1978). The predominant quaternary structure of triply liganded and most doubly liganded Hbs appears to be R-like and in particular, in ligation species 23 and 32 (Ackers *et al.*, 1992) it is thought that the third and fourth ligands bind to deoxy β subunits in a R-like quaternary structure. The R-like quaternary structure of the doubly and triply liganded Hbs may alter the tertiary structures of the unliganded subunits in a manner similar to that observed in the R-state structure of deoxyβ_4, greatly enhancing their oxygen affinity.

We are grateful to Elizabeth Getzoff, Shankari Mylvaganam and David Case for critically reading the manuscripts. This work was supported by research grants GM-40852 and HL-40453 from the National Institutes of Health. G.E.O.B. was the recipient of a predoctoral fellowship (training grant T32-GM08365) from the National Institutes of Health. The refined co-ordinates of deoxyβ_4 Hb (entry code 1CBL) have been submitted to the Brookhaven Data Bank, Brookhaven National Laboratory, Upton, NY.

References

Ackers, G. K., Doyle, M. L., Myers, D. & Daugherty, M. A. (1992). Molecular code for co-operativity. *Science*, **255**, 54–63.

Arnone, A. & Briley, P. D. (1978). Location of the heme iron atoms and characterization of the quaternary structure of the carbonmonoxy-β4 tetramer. In *Biochemical and Clinical Aspects of Hemoglobin Abnormalities* (Caughey, W. S., ed.), pp. 93–107. Academic Press, New York.

Baldwin, J. & Chothia, C. (1979). Haemoglobin: the structural changes related to ligand binding and its allosteric mechanism. *J. Mol. Biol.* **129**, 175–220.

Benesch, R. & Benesch, R. E. (1974). Homos and heteros among the hemos. *Science*, **185**, 905–908.

Borgstahl, G. E. O., Rogers, P. H. & Arnone, A. (1994). The 1·8 Å structure of carbonmonoxy-β_4 hemoglobin. Analysis of a homotetramer with the R quaternary structure of liganded $\alpha_2\beta_2$ hemoglobin. *J. Mol. Biol.* **236**, 817–830.

Dickerson, R. E. & Geis, I. (1983). *Hemoglobin* (P. Hagopian, ed.), Benjamin/Cummings Publishing Company, Inc., Menlo Park, CA.

Fermi, G., Perutz, M. F., Shaanan, B. & Fourme, R. (1984). The crystal structure of human deoxyhaemoglobin at 1·74 Å resolution. *J. Mol. Biol.* **175**, 159–174.

Gelin, B. R. & Karplus, M. (1977) Mechanism of tertiary structural changes in hemoglobin. *Proc. Nat. Acad. Sci., U.S.A.* **74**, 801–805.

Gelin, B. R., Lee, A. W.-M. & Karplus, M. (1983). Hemoglobin tertiary structural change on ligand binding: its role on the co-operative mechanism. *J. Mol. Biol.* **171**, 489–559.

Imai, K. (1979) Thermodynamic aspects of the co-operativity in four-step oxygenation equilibria of hemoglobin. *J. Mol. Biol.* **133**, 223–247.

Jack, A. & Levitt, M. (1978). Refinement of large structures by simultaneous minimization of energy and R factor. *Acta Crystallogr. sect. A*, **38**, 931–935.

Janin, J., Miller, S. & Chothia, C. (1988). Surface, subunit interfaces and interior of oligomeric proteins. *J. Mol. Biol.* **204**, 155–164.

Kavanaugh, J. S., Rogers, P. H. & Arnone, A. (1992*a*). High-resolution X-ray study of deoxy recombinant human hemoglobins synthesized from β-globins having mutant amino termini. *Biochemistry*, **31**, 8640–8647.

Kavanaugh, J. S., Rogers, P. H., Case, D. A. & Arnone, A. (1992*b*). High-resolution X-ray study of deoxyhemoglobin Rothschild 37β Trp→Arg: a mutation that creates an intersubunit chloride binding site. *Biochemistry*, **31**, 4111–4121.

Kilmartin, J. V. (1977). The Bohr effect of human hemoglobin. *Trends Biol. Sci.* **2**, 247–249.

Kitagawa, T. (1992). Investigation of higher order structures of proteins by ultraviolet resonance Raman spectroscopy. *Progr. Biophys. Mol. Biol.*, **58**, 1–18.

Kurtz, A., Rollema, H. S. & Baurer, C. (1981). Heterotropic interactions in monomeric β^{SH} chains from human hemoglobin. *Arch. Biochem. Biophys.* **210**, 200–203.

Liddington, G., Derewenda, Z., Dodson, E., Hubbard, R. & Dodson, G. (1992) High-resolution crystal structures and comparisons of T-state deoxyhaemoglobin and two liganded T-state haemoglobins: T(α-oxy) haemoglobin and T(met)haemoglobin. *J. Mol. Biol.* **228**, 551–579.

Mills, F. C. & Ackers, G. K. (1979). Quaternary enhancement in binding of oxygen by human hemoglobin. *Proc. Nat. Acad. Sci., U.S.A.* **76**, 273–277.

Nagai, K. & Kitagawa, T. (1980). Differences in Fe(II)-N_ϵ(His-F8) stretching frequencies between deoxyhemoglobins in the two alternate quaternary structures. *Proc. Nat. Acad. Sci., U.S.A.* **77**, 2033–2037.

Perutz, M. F. (1970). Stereochemistry of co-operative effects in haemoglobin. *Nature (London)*, **228**, 726–734.

Perutz, M. F. (1979). Regulation of oxygen affinity of hemoglobin: influence of structure of the globin on the heme iron. *Annu. Rev. Biochem.* **48**, 327–386.

Perutz, M. F., Fermi, G., Luisi, B., Shaanan, B. & Liddington, R. C. (1987). Stereochemistry of co-operative mechanisms in hemoglobin. *Acc. Chem. Res.* **20**, 309–321.

Phillips, S. E. V. (1980). Structure and refinement of oxymyoglobin at 1.6 Å resolution. *J. Mol. Biol.* **142**, 531–554.

Shaanan, B. (1983). Structure of oxyhaemoglobin at 2·1 Å resolution. *J. Mol. Biol.* **171**, 31–59.

Silva, M. M., Rogers, P. H. & Arnone, A. (1992). A third quaternary structure of human hemoglobin a at 1·7 Å resolution. *J. Biol. Chem.* **267**, 17248–17256.

Valdes, R. J. & Ackers, G. K. (1978). Self-association of hemoglobin β^{SH} chains is linked to oxygenation. *Proc. Natl. Acad. Sci., U.S.A.* **75**(1), 311–314.

Edited by P. E. Wright

(Received 2 September 1993; accepted 5 November 1993)